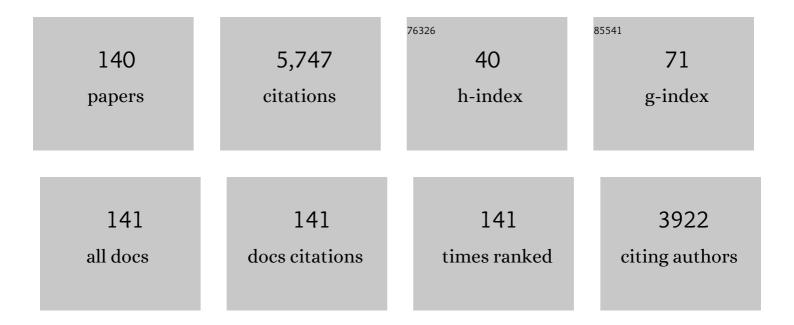
## Michael J Zehetbauer

List of Publications by Year in descending order

Source: https://exaly.com/author-pdf/1643847/publications.pdf Version: 2024-02-01



#	Article	IF	CITATIONS
1	Nanomaterials by severe plastic deformation: review of historical developments and recent advances. Materials Research Letters, 2022, 10, 163-256.	8.7	215
2	Vacancies in plastically deformed copper. International Journal of Materials Research, 2022, 96, 1044-1048.	0.3	0
3	A critical analysis of the composite model as applied to high-temperature creep of Al and an Al–Mg alloy. International Journal of Materials Research, 2022, 97, 329-335.	0.3	0
4	HPT production of large bulk skutterudites. Journal of Alloys and Compounds, 2021, 854, 156678.	5.5	12
5	Influence of shear strain on HPT-processed n-type skutterudites yielding ZT=2.1. Journal of Alloys and Compounds, 2021, 855, 157409.	5.5	17
6	Effect of high pressure torsion on crystallization and magnetic properties of Fe73.9Cu1Nb3Si15.5B6.6. Journal of Magnetism and Magnetic Materials, 2021, 525, 167679.	2.3	6
7	Enhancing the Mechanical Properties of Biodegradable Mg Alloys Processed by Warm HPT and Thermal Treatments. Materials, 2021, 14, 6399.	2.9	4
8	Anomalous Evolution of Strength and Microstructure of Highâ€Entropy Alloy CoCrFeNiMn after Highâ€Pressure Torsion at 300 and 77 K. Advanced Engineering Materials, 2020, 22, 1900752.	3.5	23
9	Half-Heusler alloys: Enhancement of ZT after severe plastic deformation (ultra-low thermal) Tj ETQq1 1 0.7843	14 rgBT /Ov	verlą <u>c</u> k 10 Tf
10	Resistivity and Thermal Expansion (4.2–820 K) of Skutterudites after Severe Plastic Deformation via HPT. Zeitschrift Fur Anorganische Und Allgemeine Chemie, 2020, 646, 1267-1272.	1.2	5
11	The Effects of Severe Plastic Deformation and/or Thermal Treatment on the Mechanical Properties of Biodegradable Mg-Alloys. Metals, 2020, 10, 1064.	2.3	14
12	Surface Analysis of Biodegradable Mg-Alloys after Immersion in Simulated Body Fluid. Materials, 2020, 13, 1740.	2.9	10
13	Phenomena Occurring in Nanostructured Stainless Steel 316LVM during Annealing under High Hydrostatic Pressure. Advanced Engineering Materials, 2019, 21, 1800101.	3.5	2
14	Exceptional Strengthening of Biodegradable Mg-Zn-Ca Alloys through High Pressure Torsion and Subsequent Heat Treatment. Materials, 2019, 12, 2460.	2.9	26
15	The Effect of Severe Plastic Deformation on Thermoelectric Performance of Skutterudites, Half-Heuslers and Bi-Tellurides. Materials Transactions, 2019, 60, 2071-2085.	1.2	21
16	The influence of crystallization conditions on the macromolecular structure and strength of Î <sup>3</sup> -polypropylene. Thermochimica Acta, 2019, 677, 131-138.	2.7	9
17	Sustainable and simple processing technique for n-type skutterudites with high ZT and their analysis. Acta Materialia, 2019, 173, 9-19.	7.9	22
18	Characterization of strain bursts in high density polyethylene by means of a novel nano creep test. International Journal of Plasticity, 2019, 116, 297-313.	8.8	7

#	Article	IF	CITATIONS
19	Strengthening during heat treatment of HPT processed copper and nickel. Materials Science & Engineering A: Structural Materials: Properties, Microstructure and Processing, 2019, 742, 124-131.	5.6	14
20	Strengthening of a Biodegradable Mg–Zn–Ca Alloy ZX50 After Processing by HPT and Heat Treatment. Minerals, Metals and Materials Series, 2018, , 277-282.	0.4	1
21	Constitution of the binary M-Sb systems (M = Ti, Zr, Hf) and physical properties of MSb2. Intermetallics, 2018, 94, 119-132.	3.9	13
22	The half Heusler system Ti <sub>1+x</sub> Fe <sub>1.33â^'x</sub> Sb–TiCoSb with Sb/Sn substitution: phase relations, crystal structures and thermoelectric properties. Dalton Transactions, 2018, 47, 879-897.	3.3	36
23	Recrystallization and grain growth of a nano/ultrafine structured austenitic stainless steel during annealing under high hydrostatic pressure. Journal of Materials Science, 2018, 53, 11823-11836.	3.7	15
24	Direct SPD-processing to achieve high-ZT skutterudites. Acta Materialia, 2018, 159, 352-363.	7.9	27
25	Rejuvenation decreases shear band sliding velocity in Pt-based metallic glasses. Materials Science & Engineering A: Structural Materials: Properties, Microstructure and Processing, 2017, 684, 517-523.	5.6	24
26	On the Half-Heusler compounds Nb1-x{Ti,Zr,Hf}xFeSb: Phase relations, thermoelectric properties at low and high temperature, and mechanical properties. Acta Materialia, 2017, 135, 263-276.	7.9	61
27	Thermal stability and latent heat of Nb–rich martensitic Ti-Nb alloys. Journal of Alloys and Compounds, 2017, 697, 300-309.	5.5	60
28	Dislocation Movement Induced by Molecular Relaxations in Isotactic Polypropylene. Macromolecules, 2017, 50, 6362-6368.	4.8	23
29	Influence of microstructure on fatigue of biocompatible β-phase Ti-45Nb. Materials Science & Engineering A: Structural Materials: Properties, Microstructure and Processing, 2017, 706, 83-94.	5.6	21
30	Mechanical properties of non-centrosymmetric CePt3Si and CePt3B. Journal of Physics Condensed Matter, 2017, 29, 185402.	1.8	5
31	Giant thermal expansion and α-precipitation pathways in Ti-alloys. Nature Communications, 2017, 8, 1429.	12.8	81
32	Ba-filled Ni–Sb–Sn based skutterudites with anomalously high lattice thermal conductivity. Dalton Transactions, 2016, 45, 11071-11100.	3.3	13
33	Mechanical properties, structural and texture evolution of biocompatible Ti–45Nb alloy processed by severe plastic deformation. Journal of the Mechanical Behavior of Biomedical Materials, 2016, 62, 93-105.	3.1	66
34	Fatigue testing method for fine bond wires in an LQFP package. Microelectronics Reliability, 2016, 64, 270-275.	1.7	9
35	Mechanical properties of half-Heusler alloys. Acta Materialia, 2016, 107, 178-195.	7.9	235
36	Producing Bulk Ultrafine-Grained Materials by Severe Plastic Deformation: Ten Years Later. Jom, 2016, 68, 1216-1226.	1.9	346

#	Article	IF	CITATIONS
37	Analysis of strain bursts during nanoindentation creep of high-density polyethylene. Polymer International, 2015, 64, 1537-1543.	3.1	8
38	In Focus - 6 <sup>th</sup> International Conference on Polymer Behavior(ICPB6). Polymer International, 2015, 64, 1505-1505.	3.1	0
39	Ba <sub>5</sub> {V,Nb} <sub>12</sub> Sb <sub>19+x</sub> , novel variants of the Ba <sub>5</sub> Ti <sub>12</sub> Sb <sub>19+x</sub> -type: crystal structure and physical properties. Physical Chemistry Chemical Physics, 2015, 17, 24248-24261.	2.8	8
40	Changes in microstructure and physical properties of skutterudites after severe plastic deformation. Physical Chemistry Chemical Physics, 2015, 17, 3715-3722.	2.8	29
41	Phase transformations and mechanical properties of biocompatible Ti–16.1Nb processed by severe plastic deformation. Journal of Alloys and Compounds, 2015, 628, 434-441.	5.5	67
42	Long-term hydrogen storage in Mg and ZK60 after Severe Plastic Deformation. International Journal of Hydrogen Energy, 2015, 40, 17144-17152.	7.1	57
43	New bulk p-type skutterudites DD0.7Fe2.7Co1.3Sb12â^'X (X = Ge, Sn) reaching ZT > 1.3. Acta Materialia, 2015, 91, 227-238.	7.9	98
44	Rate mechanism and dislocation generation in high density polyethylene and other semicrystalline polymers. Polymer, 2014, 55, 1217-1222.	3.8	13
45	n-Type skutterudites (R,Ba,Yb)yCo4Sb12 (R=Sr, La, Mm, DD, SrMm, SrDD) approaching ZTâ‰^2.0. Acta Materialia, 2014, 63, 30-43.	7.9	254
46	Enhancement of mechanical properties of biocompatible Ti–45Nb alloy by hydrostatic extrusion. Journal of Materials Science, 2014, 49, 6930-6936.	3.7	35
47	Evolution of strength and structure during SPD processing of Ti–45Nb alloys: experiments and simulations. Journal of Materials Science, 2014, 49, 6648-6655.	3.7	13
48	Effect of High-Pressure Torsion on Texture, Microstructure, and Raman Spectroscopy: Case Study of Fe- and Te-Substituted CoSb3. Journal of Electronic Materials, 2014, 43, 3817-3823.	2.2	13
49	Grain boundary excess volume and defect annealing of copper after high-pressure torsion. Acta Materialia, 2014, 68, 189-195.	7.9	51
50	Peculiarities in the Texture Formation of Intermetallic Compounds Deformed by High Pressure Torsion. Materials Research Society Symposia Proceedings, 2014, 1760, 43.	0.1	1
51	Thermoelectric properties of chalcogenide based Cu2+xZnSn1â^'xSe4. AIP Advances, 2013, 3, .	1.3	38
52	New p- and n-type skutterudites with ZT>1 and nearly identical thermal expansion and mechanical properties. Acta Materialia, 2013, 61, 4066-4079.	7.9	28
53	Nature and density of lattice defects in ball milled nanostructured copper. Mechanics of Materials, 2013, 67, 59-64.	3.2	8
54	High-Pressure Torsion to Improve Thermoelectric Efficiency of Clathrates?. Journal of Electronic Materials, 2013, 42, 1330-1334.	2.2	15

#	Article	IF	CITATIONS
55	The role of dislocations in Î <sup>3</sup> -iPP under plastic deformation investigated by X-ray line profile analysis. Mechanics of Materials, 2013, 67, 126-132.	3.2	20
56	Following the deformation behavior of nanocrystalline Pd films on polyimide substrates using in situ synchrotron XRD. Mechanics of Materials, 2013, 67, 65-73.	3.2	14
57	Effect of microstructural stability on fatigue crack growth behaviour of nanostructured Cu. Mechanics of Materials, 2013, 67, 38-45.	3.2	10
58	Correlation between the microstructure studied by X-ray line profile analysis and the strength of high-pressure-torsion processed Nb and Ta. Acta Materialia, 2013, 61, 632-642.	7.9	39
59	Dependence of thermoelectric behaviour on severe plastic deformation parameters: A case study on p-type skutterudite DD0.60Fe3CoSb12. Acta Materialia, 2013, 61, 6778-6789.	7.9	59
60	Thermal stability and phase transformations of martensitic Ti–Nb alloys. Science and Technology of Advanced Materials, 2013, 14, 055004.	6.1	107
61	Percolating porosity in ultrafine grained copper processed by High Pressure Torsion. Journal of Applied Physics, 2013, 114, 183509.	2.5	16
62	Severe Plastic Deformation, A Tool to Enhance Thermoelectric Performance. Springer Series in Materials Science, 2013, , 193-254.	0.6	14
63	Changes of Thermoelectric Properties and Hardness After HPT Processing of Micro- and Nanostructured Skutterudites. NATO Science for Peace and Security Series B: Physics and Biophysics, 2013, , 81-91.	0.3	3
64	Preface to the special issue on ultrafine-grained materials. Journal of Materials Science, 2012, 47, 7717-7718.	3.7	2
65	Spinodal decomposition in (CaxBa1â^'x)yFe4Sb12. Acta Materialia, 2012, 60, 4487-4495.	7.9	7
66	Thermoelectric properties of p-type didymium (DD) based skutterudites DDy(Fe1â^'xNix)4Sb12 (0.13⩽xâ©4	⁄20,25,) Tj	ET <u>Q</u> q0 0 0 rg
67	Effect of HPT processing on the structure, thermoelectric and mechanical properties of Sr0.07Ba0.07Yb0.07Co4Sb12. Journal of Alloys and Compounds, 2012, 537, 183-189.	5.5	71
68	The role of dislocations for the plastic deformation of semicrystalline polymers as investigated by multireflection Xâ€ray line profile analysis. Journal of Applied Polymer Science, 2012, 125, 4150-4154.	2.6	13
69	High-pressure torsion, a new processing route for thermoelectrics of high ZTs by means of severe plastic deformation. Acta Materialia, 2012, 60, 2146-2157.	7.9	117
70	Deformation twins and related softening behavior in nanocrystalline Cu–30% Zn alloy. Acta Materialia, 2012, 60, 3340-3349.	7.9	53
71	Recrystallization kinetics of ultrafine-grained Ni studied by dilatometry. Journal of Alloys and Compounds, 2011, 509, S309-S311.	5.5	23

A new generation of p-type didymium skutterudites with high ZT. Intermetallics, 2011, 19, 546-555. 72 3.9 115

#	Article	IF	CITATIONS
73	X-ray line profile analysis—An ideal tool to quantify structural parameters of nanomaterials. Jom, 2011, 63, 61-70.	1.9	42
74	Activation Enthalpies of Deformation-Induced Lattice Defects in Severe Plastic Deformation Nanometals Measured by Differential Scanning Calorimetry. Metallurgical and Materials Transactions A: Physical Metallurgy and Materials Science, 2010, 41, 810-815.	2.2	41
75	Absolute concentration of free volume-type defects in ultrafine-grained Fe prepared by high-pressure torsion. Scripta Materialia, 2010, 63, 452-455.	5.2	77
76	Bulk Nanostructured Functional Materials By Severe Plastic Deformation. Advanced Engineering Materials, 2010, 12, 692-700.	3.5	64
77	Plasticity and Grain Boundary Diffusion at Small Grain Sizes. Advanced Engineering Materials, 2010, 12, 758-764.	3.5	79
78	Determination of lamella thickness distributions in isotactic polypropylene by X-ray line profile analysis. Polymer, 2010, 51, 4195-4199.	3.8	25
79	Mechanical properties of filled antimonide skutterudites. Materials Science and Engineering B: Solid-State Materials for Advanced Technology, 2010, 170, 26-31.	3.5	92
80	Microstructure and Properties of Nanostructured Zirconium Processed by High Pressure Torsion. Materials Science Forum, 2010, 667-669, 433-438.	0.3	5
81	Thermal expansion of skutterudites. Journal of Applied Physics, 2010, 107, .	2.5	74
82	ON THE SKUTTERUDITE <font>Pt</font> <sub>4</sub> <font>Sn</font> <sub>4.4</sub> <font>Sb</font> <sub>7.6</sub> . International Journal of Modern Physics B, 2010, 24, 711-721.	2.0	4
83	Thermoelectric properties of novel skutterudites with didymium: DDy(Fe1â^'xCox)4Sb12 and DDy(Fe1â^'xNix)4Sb12. Intermetallics, 2010, 18, 57-64.	3.9	119
84	Structural and physical properties of n-type skutterudite Ca0.07Ba0.23Co3.95Ni0.05Sb12. Intermetallics, 2010, 18, 394-398.	3.9	36
85	Multifilled nanocrystalline p-type didymium – Skutterudites with ZT>1.2. Intermetallics, 2010, 18, 2435-2444.	3.9	93
86	Thermoelectric performance of mischmetal skutterudites MmyFe4â^'xCoxSb12 at elevated temperatures. Journal of Alloys and Compounds, 2010, 490, 19-25.	5.5	49
87	Impact of high pressure torsion on the microstructure and physical properties of Pr0.67Fe3CoSb12, Pr0.71Fe3.5Ni0.5Sb12, and Ba0.06Co4Sb12. Journal of Alloys and Compounds, 2010, 494, 78-83.	5.5	50
88	<i>InÂSitu</i> Probing of Fast Defect Annealing in Cu and Ni with a High-Intensity Positron Beam. Physical Review Letters, 2010, 105, 146101.	7.8	31
89	Process of intercalation of C60 with molecular hydrogen according to x-ray diffraction data. Low Temperature Physics, 2009, 35, 238-242.	0.6	9
90	Synchrotron X-ray line-profile analysis experiments for the in-situ microstructural characterisation of SPD nanometals during tensile deformation. International Journal of Materials Research, 2009, 100, 770-774.	0.3	9

#	Article	IF	CITATIONS
91	Determination of Critical Strains in Isotactic Polypropylene by Cyclic Loading-Unloading. Journal of Engineering Materials and Technology, Transactions of the ASME, 2009, 131, .	1.4	11
92	High-pressure torsion deformation of a magnesium-based nanocomposite. International Journal of Materials Research, 2009, 100, 906-909.	0.3	3
93	Microstructure and fatigue properties of the ultrafine-grained AM60 magnesium alloy processed by equal-channel angular pressing. Materials Science & Engineering A: Structural Materials: Properties, Microstructure and Processing, 2009, 503, 176-180.	5.6	74
94	High thermoelectric performance of triple-filled <i>n</i> -type skutterudites (Sr,Ba,Yb) <sub><i>y</i></sub> Co <sub>4</sub> Sb <sub>12</sub> . Journal Physics D: Applied Physics, 2009, 42, 225405.	2.8	63
95	Influence of post-deformation on CP-Ti processed by equal channel angular pressing. Materials Science & Engineering A: Structural Materials: Properties, Microstructure and Processing, 2008, 476, 98-105.	5.6	81
96	The presence and nature of vacancy type defects in nanometals detained by severe plastic deformation. Materials Science & Engineering A: Structural Materials: Properties, Microstructure and Processing, 2008, 493, 116-122.	5.6	186
97	The Innovation Potential of Bulk Nanostructured Materials. Advanced Engineering Materials, 2007, 9, 527-533.	3.5	183
98	Vacancy production during plastic deformation in copper determined by in situ X-ray diffraction. Materials Science & Engineering A: Structural Materials: Properties, Microstructure and Processing, 2007, 462, 398-401.	5.6	83
99	Monodispersed nanocrystalline Co1–xZnxFe2O4 particles by forced hydrolysis: Synthesis and characterization. Journal of Magnetism and Magnetic Materials, 2007, 311, 46-50.	2.3	88
100	Non-microscopical methods for characterization of microstructures and properties of UFG metals. International Journal of Materials Research, 2007, 98, 290-298.	0.3	2
101	Deformation Induced Vacancies with Severe Plastic Deformation: Measurements and Modelling. Materials Science Forum, 2006, 503-504, 57-64.	0.3	97
102	SPD Processed Alloys as Efficient Vacancy-Hydrogen Systems. Solid State Phenomena, 2006, 114, 177-182.	0.3	17
103	On the Microstructure of HPT Processed Cu under Variation of Deformation Parameters. Materials Science Forum, 2006, 503-504, 51-56.	0.3	21
104	Metallic Nano-Materials and Nanostructures: Development of Technology Roadmap. Solid State Phenomena, 2006, 114, 345-0.	0.3	6
105	Spatial fluctuations of the microstructure during deformation of Cu single crystals. Zeitschrift Für Kristallographie, Supplement, 2006, 2006, 105-110.	0.5	3
106	Structural methods for studying nanocrystalline materials. Journal of Magnetism and Magnetic Materials, 2005, 294, 152-158.	2.3	10
107	Vacancies in plastically deformed copper. International Journal of Materials Research, 2005, 96, 1044-1048.	0.8	18
108	Vacancy concentrations determined from the diffuse background scattering of X-rays in plastically deformed copper. International Journal of Materials Research, 2005, 96, 578-583.	0.8	33

#	Article	IF	CITATIONS
109	Footprints of deformation mechanisms during in situ x-ray diffraction: Nanocrystalline and ultrafine grained Ni. Applied Physics Letters, 2005, 86, 231910.	3.3	19
110	Investigation of the Microstructural Evolution During Large Strain Cold Working of Metals by Means of Synchrotron Radiation—A Comparative Overview. Journal of Engineering Materials and Technology, Transactions of the ASME, 2002, 124, 41-47.	1.4	13
111	Large strain work hardening in the alloy Al–1Mg–1Mn at low and intermediate deformation temperatures: experiments and modelling. Materials Science & Engineering A: Structural Materials: Properties, Microstructure and Processing, 2002, 324, 244-250.	5.6	12
112	Ultrafine-grained microstructures evolving during severe plastic deformation. Jom, 2000, 52, 34-36.	1.9	18
113	Scanning X-ray diffraction peak profile analysis in deformed Cu-polycrystals by synchrotron radiation1This work is dedicated to Professor Dr Guenther Schoeck on the occasion of his 70th birthday.1. Acta Materialia, 1999, 47, 1053-1061.	7.9	54
114	Large-strain hardening curves corrected for texture development. Modelling and Simulation in Materials Science and Engineering, 1999, 7, 875-891.	2.0	14
115	Microstructural Parameters in Large Strain Deformed Ni Polycrystals as Investigated by Synchrotron Radiation. Physica Status Solidi A, 1999, 175, 501-511.	1.7	17
116	Measurements and Evaluation of Strain Rate Sensitivity in Al at Late Stages of Deformation. Materials Science Forum, 1997, 242, 147-152.	0.3	1
117	Dislocation densities and internal stresses in large strain cold worked pure iron. Materials Science & Engineering A: Structural Materials: Properties, Microstructure and Processing, 1997, 234-236, 445-448.	5.6	38
118	Characteristics of work hardening in late stages of high temperature deformation of aluminium single crystals. Physica Status Solidi A, 1996, 157, 265-273.	1.7	10
119	Characteristics of low temperature serrated flow in CuBe alloy. Physica Status Solidi A, 1996, 157, 295-302.	1.7	3
120	Measurement of Dislocation Density by Residual Electrical Resistivity. Materials Science Forum, 1996, 210-213, 133-140.	0.3	25
121	Model calculations of large strain strengthening characteristics of commercially pure b.c.c. iron. Physica Status Solidi A, 1995, 151, 305-311.	1.7	8
122	Dislocation resistivity in Cu: dependence of the deviations from Matthiessen's rule on temperature, dislocation density and impurity content. Journal of Physics Condensed Matter, 1995, 7, 3515-3528.	1.8	12
123	Dislocation Density and Long Range Internal Stresses in Heavily Cold Worked Cu Measured by X-ray Line Broadening. International Journal of Materials Research, 1995, 86, 827-831.	0.3	6
124	Evolution of Microstructural Parameters in Large Strain Deformation: Description by Zehetbauer's Model. Key Engineering Materials, 1994, 97-98, 335-340.	0.4	27
125	Effects of Non-Equilibrium Vacancies on Strengthening. Key Engineering Materials, 1994, 97-98, 287-306.	0.4	35
126	Onset mechanisms of discontinuous flow at low temperatures in one- and two-phase Cuî—,Be alloys. Materials Science & Engineering A: Structural Materials: Properties, Microstructure and Processing, 1993, 164, 240-245.	5.6	11

#	Article	IF	CITATIONS
127	Cold work hardening in stages IV and V of F.C.C. metals—I. Experiments and interpretation. Acta Metallurgica Et Materialia, 1993, 41, 577-588.	1.8	248
128	Cold work hardening in stages IV and V of F.C.C. metals—II. Model fits and physical results. Acta Metallurgica Et Materialia, 1993, 41, 589-599.	1.8	188
129	Calorimetric study of defect annihilation in low temperature-deformed pure Zn. Scripta Metallurgica Et Materialia, 1991, 25, 559-564.	1.0	10
130	Deviations from Matthiessen's rule in copper containing dislocations. Solid State Communications, 1991, 79, 465-468.	1.9	3
131	Theory and experiment on deviations of Matthiessen's rule in dislocated crystals: a constructive reply. Journal of Physics Condensed Matter, 1989, 1, 2833-2841.	1.8	7
132	Effects of stress-aided static recovery in iteratively cold-worked aluminium and copper. Materials Science and Engineering, 1987, 89, 93-101.	0.1	26
133	Electrical resistivity of dislocations in aluminum. Physical Review B, 1985, 31, 1172-1173.	3.2	11
134	Variations of microstructure in large strain cold-rolled pure aluminium. Scripta Metallurgica, 1985, 19, 505-510.	1.2	12
135	Determination of sro parameters of α-AgAl from resistivity measurement. Acta Metallurgica, 1984, 32, 1053-1060.	2.1	10
136	Microhardness and yield stress of cold rolled pure aluminum up to very high deformation. Scripta Metallurgica, 1983, 17, 221-226.	1.2	9
137	On the Mechanism of Domain Refinement due to Scratching. Japanese Journal of Applied Physics, 1982, 21, L580-L582.	1.5	10
138	Heterogeneous short-range order as an origin of the K-state in α-FeAl. Physica Status Solidi A, 1980, 62, 213-222.	1.7	18
139	Effect of high deformatio of electrical resistivity in pure aluminium. Scripta Metallurgica, 1980, 14, 1125-1128.	1.2	14
	Enhanced Thermoelectric Figure of Merit in P-Type		

Enhanced Thermoelectric Figure of Merit in P-Type DD<sub&gt;y&lt;/sub&gt;(Fe&lt;sub&gt;1-X&lt;/sub&gt;Co&lt;sub&gt;x&lt;/sub&gt;)&lt;sub&gt;4&lt;/sub&gt;Sb&**dt;3**ub>**d**</sub Solid State Phenomena, 0, 170, 240-243. 140